NANO LETTERS

Letter

pubs.acs.org/NanoLett

Scaling Limits of Graphene Nanoelectrodes

Syed Ghazi Sarwat, Pascal Gehring, Gerardo Rodriguez Hernandez, Jamie H. Warner, G. Andrew D. Briggs, Jan A. Mol, and Harish Bhaskaran*

Department of Materials, University of Oxford, Oxford, OX1 3PH, United Kingdom

Supporting Information

ABSTRACT: Graphene nanogap electrodes have been of recent interest in a variety of fields, ranging from molecular electronics to phase change memories. Several recent reports have highlighted that scaling graphene nanogaps to even smaller sizes is a promising route to more efficient and robust molecular and memory devices. Despite the significant interest, the operating and scaling limits of these electrodes are completely unknown. In this paper, we report on our observations of consistent voltage driven resistance switching in sub-5 nm graphene nanogaps. We find that such electrical switching from an insulating state to a conductive state occurs at very low currents and voltages (0.06 μA and 140 mV), independent of the conditions (room ambient, low temperatures, as well as in vacuum), thus portending potential limits to scaling of functional devices with carbon electrodes. We then associate this phenomenon to the formation and rupture of carbon chains. Using a phase change material in the nanogap as a demonstrator device, fabricated using a self-alignment technique, we show that for gap sizes approaching 1 nm the switching is dominated by such carbon chain formation, creating a fundamental scaling limit for potential devices. These findings have important implications, not only for fundamental science, but also in terms of potential applications.

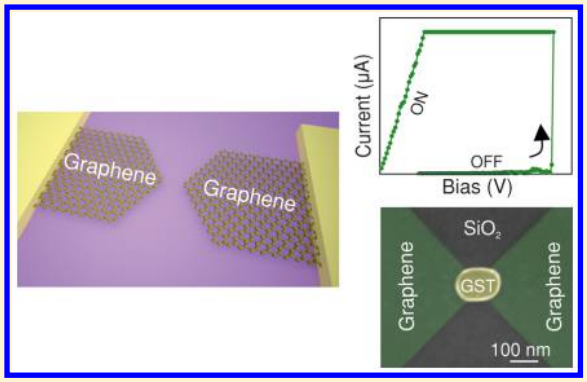

KEYWORDS: *Graphene nanogaps, electroburning, phase change material, self-alignment approach*

The ability to create nanometer-sized gaps in sp^2-bonded carbon materials offers a means of contacting nanoscale objects, for example, nanocrystals and single molecules, that cannot be achieved with conventional metallic electrodes. The fact that these materials have a thickness of only a single or few atomic bond lengths strongly reduces electrostatic screening and enables gating of molecular orbitals.[1] Moreover, the reduced contact area between atomically thin electrodes and phase change material nanocrystals has been shown to lower the power requirements for current-induced phase changes.[2] Because of the strength of the sp^2 carbon−carbon bond, the atomic mobility of carbon atoms is significantly lower than that of metal atoms, and carbon-based electrodes are therefore expected to be significantly more robust, even at room temperature.[3] However, we find that the intense electric fields generated by applying a bias voltage across a nanometer-size graphene gap result in the spontaneous rearrangement of atoms and bonds that lead to reversible switching of the resistance. Here, we investigate the scaling limits imposed by this switching behavior in the context of phase change memory (PCM) devices. However, our findings carry equal significance for all applications based on graphene nanogaps, including single-molecule electronics[1,4,5] and graphene-based genome sequencing.[6]

The energy consumption and access speed of phase change memories[2] and other data storage technologies, including oxide memory,[7,8] have been shown to improve significantly as a result of scaling down the dimensions between the contact electrodes. Ultimately, the performance of these memory devices is determined by the active volume that switches between two states of contrasting electrical resistance. In theory, this volume could be scaled to the dimension of a single unit cell volume[9] that requires sub-2 nm spaced electrodes. In this paper, we find that it is the intrinsic switching behavior of the graphene electrodes, rather than the properties of the phase change material, that ultimately limits the device scaling and therefore its performance.

We use a method of feedback-controlled electroburning to create graphene nanogaps ranging from ∼1 to 60 nm and, using a self-alignment approach, we deposit a small volume of $Ge_2Sb_2Te_5$ (GST) over the gap. Only in the case of large nanogaps (>20 nm) do we find that the resistance switching is due to the GST, while for smaller gaps it is fully dominated by the graphene. We characterize the graphene switching by studying bare graphene nanogaps and estimate the critical electric field for switching F_{crit} = 40 mV/Å. This critical field dictates the maximum operating voltage for a given gap-size, or minimum gap-size for a given operating voltage, for any technology based on graphene nanoelectrodes.

Received: March 2, 2017
Revised: May 7, 2017
Published: May 8, 2017

DOI: 10.1021/acs.nanolett.7b00909
Nano Lett. 2017, 17, 3688−3693

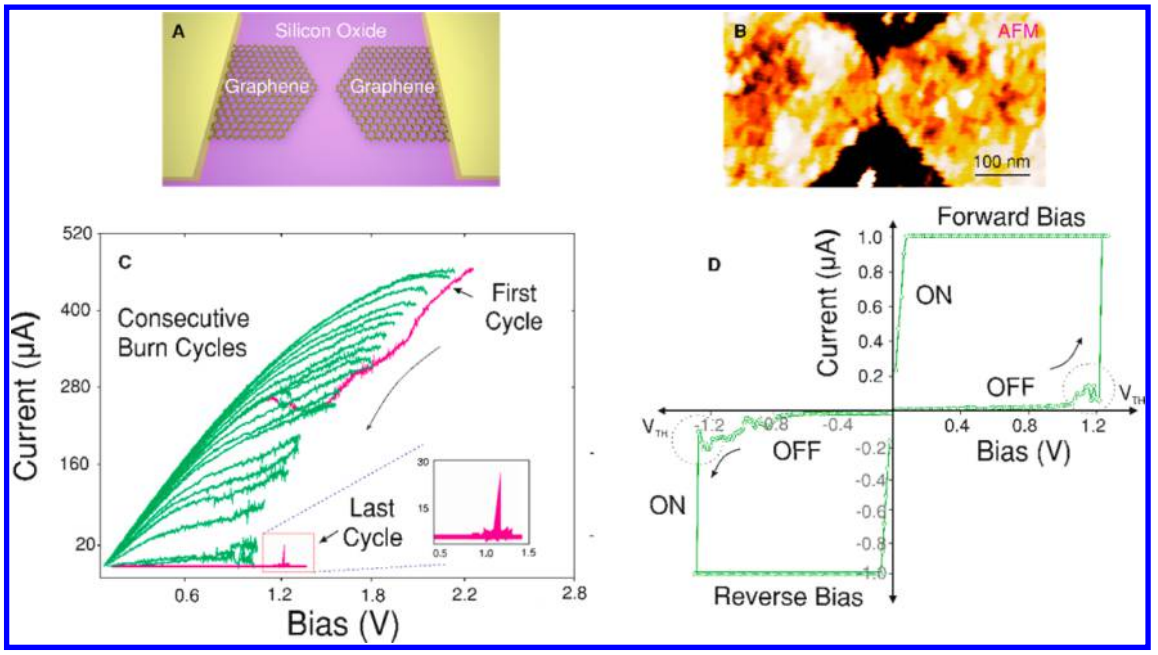

Figure 1. A graphene nanogap device. (A) Schematic representation of a graphene nanogap device; gap size is exaggerated for visualization. (B) AFM image of a graphene nanogap device; the gap (~1 nm) is not resolvable near the center of the constriction. (C) Current−voltage (I−V) characteristics during feedback-controlled electroburning of graphene in ambient conditions. Inset represents the last cycle of the burning process, which shows a spike in conductance just before the gap forms. This current spike is attributed to single carbon filament formation. (D) Low-bias switching of a graphene nanogap device (3 nm gap size) in ambient conditions. The first quadrant represents switching with a forward (positive) bias. The device switched from a high resistive state to a low resistive state in ambient conditions at a switching voltage of 1.22 V and current 60 nA. The third quadrant shows the current−voltage characteristics of the same device under reverse (negative) polarity. The device switched at a voltage of 1.28 V and current of 100 nA. For all reversible switching experiments, a current compliance of 1000 nA was used.

We use a feedback-controlled electroburning[1,10] technique that relies on controlled Joule heating to form a nanoscale gap between two electrodes in an appropriately patterned graphene ribbon. This method has previously been used to create sub-5 nm gaps in mechanically exfoliated graphene,[1] chemical vapor deposition (CVD) grown graphene,[10,11] and epitaxial graphene.[12] Here, we use this method to create nanogaps in 2−3 layer CVD-grown graphene that was transferred onto a Si/300 nm SiO_2 substrate with Au connectors and bond pads prefabricated on the substrate. We use few-layered graphene rather than single-layer graphene in order to limit the effects of defects induced by sputter deposition of GST.[13] The graphene was patterned into a bow-tie geometry with a 100 nm wide constriction (see Figure 1B) using electron beam lithography and oxygen-plasma etching. During the electroburning process, nanogaps form at the constriction, where the current density and therefore the Joule heating are highest.[10] At each stage of the electroburning process, we monitor the source-drain current when the voltage across the device is ramped up (see Figure 1C). As the current drops due to electroburning of graphene at the constriction, the resistance increases; the feedback-control is programmed to then ramp down the applied bias voltage back to zero. This process is repeated until the device has a resistance >500 MΩ. By adjusting the feedback-control parameters, we can fabricate nanogaps ranging from approximately 1 to 100 nm.

We estimate the size of the nanogaps by fitting the measured current−voltage curve to the Simmons model.[14] From these fits (see Section S2) we find that the smallest gaps range from 0.5 to 3.5 nm. Using atomic force microscopy (AFM) we confirm that the nanogap formation starts at the corners of the constriction and then propagates inward (see Figure 1B). In approximately half of the devices, we observe a sharp increase in the conductance prior to the formation of a nanogap (see inset Figure 1C). Similar conductance enhancement behavior has been reported before[15−17] and is attributed to the formation of carbon filaments. Density functional theory and tight-binding simulations have shown that the transition from a multipath configuration to a single-path configuration may lead to an enhancement of quantum transport.[17] In the following section, we describe the observation of reversible resistance switching in our devices, which we attribute to the controlled formation of carbon filaments.

After we form a nanogap using feedback-controlled electroburning, we can set the device back to its low resistance state by sweeping the bias voltage past a threshold voltage in ambient conditions (see Figure 1D). We observe that this switching behavior is independent of the bias polarity after having switched the device from the high resistive "OFF" to the low resistive "ON" state and by applying a forward bias we switch it OFF by repeating the electroburning and then switch it ON again by applying a negative bias. As shown in Figure 2B, the conductance switching is fully reversible; we can switch the device from the ON to the OFF state by performing the feedback-controlled electroburning process (see Figure 2C) and switch back from the OFF to the ON state by sweeping the bias voltage beyond the threshold voltage (Figure 2D). We can repeat SET (from OFF to ON) and RESET (from ON to OFF) multiple times.

Reversible conductance switching of graphene nanogaps has previously been reported for graphene on SiO_2 and suspended graphene in vacuum.[18−20] The temperature dependence observed in these studies, as well as in this paper (see Figure S4d) provides a strong indication that the switching process

DOI: 10.1021/acs.nanolett.7b00909
Nano Lett. 2017, 17, 3688−3693

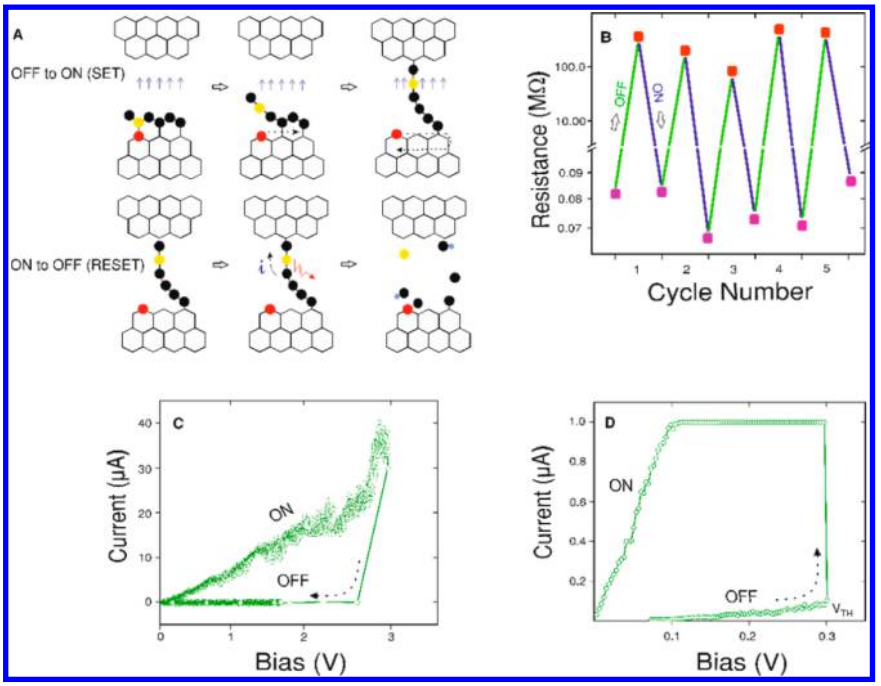

Figure 2. Cyclic switching via filamentation in a graphene nanogap device. (A) Proposed scheme for the formation and breaking of carbon filaments following ref 21. During SET (OFF to ON), formation of a carbon filament initiates from the edge of the graphene; when the local electric field at atomically sharp edges gets sufficiently high, it breaks a bond parallel to the axial electric field (between red and yellow atoms in the schematic). Filamentation then proceeds in a row-by-row fashion as indicated by the dashed arrows. For RESET (ON to OFF), Joule heating provides sufficient thermal energy for the rupture of bonds through oxidation of carbon atoms (oxygen represented by blue circles). (B) The device is switched between the high resistance and low resistance state multiple times in ambient conditions. (C) Current−voltage behavior during RESET in ambient conditions showing similarity to electroburning traces in the previous electroburning cycle (Figure 1c). (D) Illustrates a typical SET $I-V$ characteristic in ambient conditions. The device switched at a switching voltage of 300 mV and current 80 nA.

involves the rearrangement of atoms and/or chemical bonds that requires overcoming a barrier.[18] A possible mechanism for this rearrangement is the formation of carbon filaments, which in the case of carbon nanotubes was identified as the process through which they unravel by the action of an electric field.[21] Figure 2A shows a schematic depiction of the filamentation process; the force exerted by the electric field breaks the C—C bond of an edge atom with incomplete sp^2 bonding. The filamentation process then proceeds as a rupture of C—C bonds parallel to the graphene edge. The fact that we observe reversible switching in ambient conditions is potentially because of the feedback-control when switching the device OFF. The gap size resulting from electroburning without feedback-control strongly depends on the oxygen concentration of the atmosphere and ranges between ∼100 nm in ambient condition to ∼5 nm under a vacuum ∼10^{-5} mbar.[22] We find that we are unable to SET devices when electroburning without feedback-control.

The SET requires a field strength F_{crit} = 40 mV/Å by assuming to a first approximation that the applied bias voltage drops linearly across the 0.75 nm gap. This field strength is similar to that observed previously[19] for a gap size of ∼10 nm, which switched at ∼4 V, suggesting that there is a critical field strength required to unzip the carbon filament(s) from graphene. Interestingly, this electric field strength is 2 orders of magnitude lower than the field strength that has been theoretically estimated (≥2 V/Å)[23,24] for unravelling a carbon filament from a graphene edge. We attribute this discrepancy to weakening of the C—C bond strength resulting from incomplete sp^2 hybridization and enhancement of the local electric field at atomically sharp graphene edges.[25]

On the basis of measurements of the critical field required for switching graphene, we estimate that to switch a $Ge_2Sb_2Te_5$ (GST) volume with a voltage less than 4 V, we require a gap size of at least 10 nm. To demonstrate this, we compare GST contacted in both 1 and 20 nm wide graphene nanogaps. To place the GST volume over the graphene nanogap, we use a self-alignment method that relies on the local removal of PMMA in the vicinity of the graphene constriction during the electroburning process. Similar self-alignment techniques have been previously demonstrated for fabrication of CNT nanogaps-based PCM devices,[26] however, not in combination with feedback-controlled electroburning. Here we demonstrated the applicability of this technique on CVD grown graphene, which allows for scalability as graphene can be grown on wafers and subsequently patterned using lithography. The simplified one-step process requires no high-resolution lithography or vacuum. After several cycles of electroburning, we spin-coated ∼100 nm of poly(methyl methacrylate) (PMMA) onto our devices. Continuing the feedback-controlled electroburning process, we locally heat up the graphene constriction, which leads to the formation of trenches resulting from the local evaporation of PMMA. These trenches serve as self-aligned windows for subsequent deposition of the phase change material, which in our demonstrator case is GST. The size of the trenches depends on the number of electroburning cycles, that is, the resistance of the graphene device, prior to spinning the resist. We have simulated the electroburning process (see Section S3) using finite element analysis. The resulting trench sizes agree well with our experimental observations. Figure 3A,B shows an AFM image of a self-aligned trench in PMMA, and a scanning electron microscopy (SEM) image of the device after sputter-

DOI: 10.1021/acs.nanolett.7b00909
Nano Lett. 2017, 17, 3688−3693

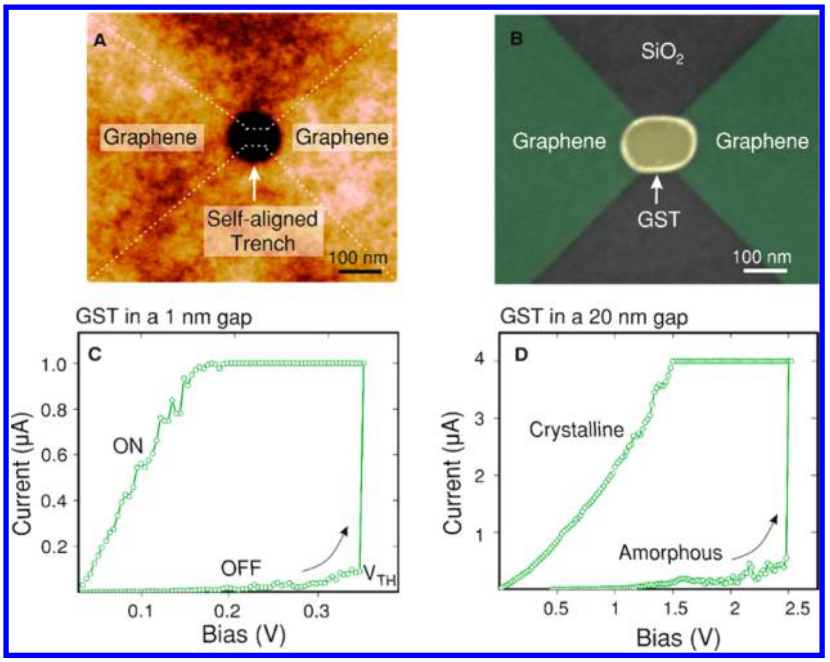

Figure 3. Self-alignment approach and phase change memory device. (A) AFM image showing a trench of size 148 nm (largest lateral dimension) in PMMA. This trench is formed in situ from local degradation of PMMA due to Joule heating during the electroburning process. Dotted line outlines the graphene ribbon underneath PMMA. (B) Colored SEM image of a self-aligned PCM device showing the phase change material (GST) in the nanogap. The trench in the PMMA ensures that the GST is self-aligned to the gap in the graphene electrodes, thus eliminating the need for sub-10 nm alignment. (C) Current−voltage trace of a GST nanogap device; GST is aligned to make contact to graphene in a 1 nm nanogap. The device switches from a high resistive state to a low resistive state in ambient conditions at a switching voltage of 370 mV and current 100 nA. (D) Current−voltage characteristics of a GST device with a gap size of ∼20 nm. GST switches from a highly resistive amorphous state to a less resistive crystalline state at a bias of 2.5 V and current 500 nA. The ratio of resistance between these states averages to ∼1000.

deposition of GST (∼12 nm) and PMMA lift-off. We avoided capping layers in order to eliminate any probable interfacial interactions between the capping layer and GST, which are known to influence switching behavior.[27]

Figure 3C shows the current−voltage characteristics of a self-aligned PCM device in a 1 nm wide nanogap. The device switches from a highly resistive state to a low resistive state at ∼2.5 V (Figure 3D) similar to the observed switching in bare graphene nanogaps in Figure 2A,B. GST is a semiconductor in both its amorphous and crystalline states, and we therefore do not expect to observe a linear $I-V$ character in either the ON and the OFF state. However, the $I-V$ characteristics of the ON state of the GST in a 1 nm gap is linear, similar to the bare nanogap. From this, we infer that the switching in the 1 nm nanogap is dominated by the formation of carbon filaments. By contrast, for GST deposited in a 20 nm gap the $I-V$ characteristics shows an exponential dependence in both the ON and the OFF state, which is in agreement with previous measurements of GST. Switching in GST devices occurs at a relatively high power and the resistance ratio between the highly resistive and less resistive state is ∼1000, indicative of switching in GST.[4,15] Finally, we test a device with a ∼ 20 nm nanogap without GST and find that the device has an open circuit characteristics, displaying no switching behavior even at very large bias values. At very large voltages of ∼120−150 V, dielectric breakdown of the underlying SiO_2 substrate is seen to occur (see Figure S4a). We attribute the absence of filamentation in wider gaps to instabilities of long carbon filaments.[28,29]

Reversible conductance switching has also been observed in SiO_2-based devices. To exclude effects[7,8] of SiO_2 mediated conductance switching we carried-out two experiments. In the first experiment, we placed 15 nm thick SiO_2 in the sub-4 nm gaps using the self-alignment technique. We observed no switching behavior, other than dielectric breakdown at ∼10 V (see Figure S4b). In the second, we created graphene nanogaps on an SiN substrate (see Figure S 5d), a material that shows no intrinsic switching.[8] We observed a similar switching behavior on this substrate as observed on the SiO_2 substrate. Furthermore, formation of Si nanoclusters through reduction of SiO_2 is recognized as the mechanism behind resistance switching in SiO_2 switching. Therefore, an oxygen deficient atmosphere is a prerequisite[7,8] for switching in unpassivated SiO_2. Our devices can be switched both ways readily in ambient conditions. It is therefore highly unlikely that SiO_2 switches in our devices because the switching site, which is the surface, is exposed to an oxygen rich atmosphere. In addition, the ratio of resistance between the OFF and the ON state is typically[7,8,30] > 10^4 in SiO_2, which is an order magnitude more than observed in our devices.

Having thus established sufficient evidence for switching from carbon filament(s) formation in nanogaps, an important question is how filamentation is possible when the phase change materials we use ($Ge_2Sb_2Te_5$ or GST) fills the 0.75 nm gap. The answer lies in structuring of the GST film during sputter deposition. Chalcogenide (which GST is) atoms show strong bonding preference for each other over SiO_2 for reasons relating to minimization of strain and surface energies and in the case of GST on SiO_2, this results in poor adhesion with the SiO_2 substrate.[31] Thus, it is expected that the island growth mode or the Volmer−Weber mode is preferred over layer by layer growth mode during deposition.[32] Furthermore, graphene shows a catalytic property toward the growth of chalcogenides.[33] This would result in the GST islands on graphene

DOI: 10.1021/acs.nanolett.7b00909
Nano Lett. 2017, 17, 3688−3693

growing in all directions bridging, but not filling, the gap. This is supported by the absence of switching in the graphene nanogaps with SiO_2 in the gap. Furthermore, we deduce from experiments (see Figure S6) that for a 1 nm gap, GST should switch at ~2.15 V. However, switching in GST-bridged sub-5 nm devices occurs mostly at $V_T \sim 0.6$ V (with standard deviation of 0.5 V), which is similar to observed in empty graphene nanogaps. This strongly supports the argument that the presence of sputtered GST does not influence the switching behavior. Thus, there is a clear indication that regardless of the switching mechanism, there is a fundamental limit to scaling graphene nanogaps for such relevant material systems. This perhaps also applies for carbon nanotube nanogaps, which share similar bonding configuration (sp^2) as graphene and could be a subject of future work. Importantly, molecular electronics where the actual gap is not filled entirely by the molecule, but has several areas where such chains can grow, might also have a similar scaling limit.

Therefore, our observations indicate resistance switching in graphene nanogaps, which we attribute to the controlled formation and breakdown of carbon filaments. Analyzing the switching behavior, we find that the formation of carbon filaments is electric field dependent and only occurs in sub-5 nm gaps. These experiments demonstrate for the first time, reversible resistance switching in graphene nanogaps in ambient conditions. For PCM devices with electrode separations less than 5 nm, we find the resistance switching to be fully dominated by the formation of carbon filaments. Whereas the actual mechanisms that we propose (carbon filamentation) need further unambiguous proof, nonetheless our results point toward a key scaling limit to using such electrodes.

Thus, electric-field driven resistance switching in graphene nanogaps constrains the operational voltages possible in such devices. We find that at room temperature, switching can occur at $V_{th} < 0.4$ V, which, for example, is the typical operating voltage for single-molecule devices. The noise typically observed in graphene-based single-molecule transistors at room temperature is likely to be the result of rearrangement of atoms and bonds at the edges of the electrodes. Our results highlight the importance of gaining better knowledge of the edge chemistry in graphene nanogaps. These initial findings need further investigation by research groups specializing in techniques such as atomic-scale imaging to verify the nature of these atomic chains, as well as the influence of the actual material in the gap on the formation of these chains.

Although the potential formation of graphene filaments poses challenges to the development of graphene-based nanoelectrodes, it also offers exciting opportunities to study charge transport in atomic carbon chains. The formation of carbon chains (cumulene and polyyne chains) have been observed using transmission electron microscopy.[34] If these structures could be controllably formed between graphene nanoelectrodes, they could serve as a test bed for the observation of a plethora of transport phenomena predicted in atomic chains[28,29,35] and could further also be extended for various applications such as all carbon-based transistors.

■ ASSOCIATED CONTENT

Supporting Information

The Supporting Information is available free of charge on the ACS Publications website at DOI: 10.1021/acs.nanolett.7b00909.

Device fabrication and electrical characterization, tunneling current fitting model, finite elemental analysis, switching characteristics in more devices, gap size-dependent scaling behavior of GST's threshold voltage (PDF)

■ AUTHOR INFORMATION

Corresponding Author

*E-mail: harish.bhaskaran@materials.ox.ac.uk.

ORCID

Jamie H. Warner: 0000-0002-1271-2019
Jan A. Mol: 0000-0003-0411-2598
Harish Bhaskaran: 0000-0003-0774-8110

Notes

The authors declare no competing financial interest.

■ ACKNOWLEDGMENTS

S.G.S acknowledges a Felix Scholarship that supports his Doctor of Philosophy. J.M. acknowledges an RAEng Fellowship. All authors acknowledge support from EPSRC via the Manufacturing Fellowship EP/J018694/1 as well as the WAFT collaboration (EP/M015173/1).

■ REFERENCES

(1) Prins, F.; et al. Room-Temperature Gating of Molecular Junctions Using Few-Layer Graphene Nanogap Electrodes. *Nano Lett.* **2011**, *11*, 4607−461.
(2) Xiong, F.; Liao, A. D.; Estrada, D.; Pop, E. Low-Power Switching of Phase-Change Materials with Carbon Nanotube Electrodes. *Science* **2011**, *332*, 568−570.
(3) Lörtscher, E. Wiring molecules into circuits. *Nat. Nanotechnol.* **2013**, *8*, 381−4.
(4) Mol, J. A.; et al. Graphene-porphyrin single-molecule transistors. *Nanoscale* **2015**, *7*, 13181−13185.
(5) Lau, C. S.; et al. Redox-Dependent Franck−Condon Blockade and Avalanche Transport in a Graphene−Fullerene Single-Molecule Transistor. *Nano Lett.* **2016**, *16*, 170−176.
(6) Heerema, S. J.; Dekker, C. Graphene nanodevices for DNA sequencing. *Nat. Nanotechnol.* **2016**, *11*, 127−136.
(7) He, C.; et al. Multilevel resistive switching in planar graphene/SiO_2 nanogap structures. *ACS Nano* **2012**, *6*, 4214−4221.
(8) Yao, J.; Sun, Z.; Zhong, L.; Natelson, D.; Tour, J. M. Resistive Switches and Memories from Silicon Oxide. *Nano Lett.* **2010**, *10*, 4105−4110.
(9) Loke, D.; et al. Breaking the speed limits of phase-change memory. *Science* **2012**, *336*, 1566−1569.
(10) Lau, C. S.; Mol, J. a.; Warner, J. H.; Briggs, G. a. D. Nanoscale control of graphene electrodes. *Phys. Chem. Chem. Phys.* **2014**, *16*, 20398−20401.
(11) Nef, C.; et al. High-yield fabrication of nm-size gaps in monolayer CVD graphene. *Nanoscale* **2014**, *6*, 7249−7254.
(12) Ullmann, K.; et al. Single-Molecule Junctions with Epitaxial Graphene Nanoelectrodes. *Nano Lett.* **2015**, *15*, 3512−3518.
(13) Behnam, A.; et al. Nanoscale phase change memory with graphene ribbon electrodes. *Appl. Phys. Lett.* **2015**, *107*, 123508.
(14) Simmons, J. G. Generalized Formula for the Electric Tunnel Effect between Similar Electrodes Separated by a Thin Insulating Film. *J. Appl. Phys.* **1963**, *34*, 1793.
(15) Barreiro, A.; Börrnert, F.; Rümmeli, M. H.; Büchner, B.; Vandersypen, L. M. K. Graphene at High Bias: Cracking, Layer by Layer Sublimation, and Fusing. *Nano Lett.* **2012**, *12*, 1873−1878.
(16) Lu, Y.; Merchant, C. A.; Drndić, M.; Johnson, A. T. C. In situ electronic characterization of graphene nanoconstrictions fabricated in a transmission electron microscope. *Nano Lett.* **2011**, *11*, 5184−5188.

DOI: 10.1021/acs.nanolett.7b00909
Nano Lett. 2017, 17, 3688−3693

(17) Sadeghi, H.; et al. Conductance enlargement in picoscale electroburnt graphene nanojunctions. *Proc. Natl. Acad. Sci. U. S. A.* **2015**, *112*, 2658−2663.
(18) Zhang, H.; et al. Visualizing electrical breakdown and ON/OFF states in electrically switchable suspended graphene break junctions. *Nano Lett.* **2012**, *12*, 1772−1775.
(19) Standley, B.; et al. Graphene-based atomic-scale switches. *Nano Lett.* **2008**, *8*, 3345−3349.
(20) Li, Y.; Sinitskii, A.; Tour, J. M. Electronic two-terminal bistable graphitic memories. *Nat. Mater.* **2008**, *7*, 966−971.
(21) Rinzler, A. G.; et al. Unraveling Nanotubes - Field-Emission from an Atomic Wire. *Science* **1995**, *269*, 1550−1553.
(22) Marquardt, C. W.; et al. Electroluminescence from a single nanotube-molecule-nanotube junction. *Nat. Nanotechnol.* **2010**, *5*, 863−867.
(23) Huang, H.; Li, Z.; Wang, W.; Kreuzer, H. J. nanoribbons. *27th Int. Vac. Nanoelectron. Conf.* **2014**, 2−3.
(24) Ghosh, D.; Chen, S. Solid-state electronic conductivity of ruthenium nanoparticles passivated by metal−carbon covalent bonds. *Chem. Phys. Lett.* **2008**, *465*, 115−119.
(25) Wang, H. M.; et al. Fabrication of graphene nanogap with crystallographically matching edges and its electron emission properties. *Appl. Phys. Lett.* **2010**, *96*, 023106.
(26) Xiong, F.; et al. Self-Aligned Nanotube − Nanowire Phase Change Memory. *Nano Lett.* **2013**, *13*, 464−469.
(27) Simpson, R. E.; et al. Toward the Ultimate Limit of Phase Change in $Ge_2Sb_2Te_5$. *Nano Lett.* **2010**, *10*, 414−419.
(28) Banhart, F. Chains of carbon atoms: A vision or a new nanomaterial? *Beilstein J. Nanotechnol.* **2015**, *6*, 559−569.
(29) Jin, C.; Lan, H.; Peng, L.; Suenaga, K.; Iijima, S. Deriving Carbon Atomic Chains from Graphene. *Phys. Rev. Lett.* **2009**, *102*, 205501.
(30) Fowler, B. W.; et al. Electroforming and resistive switching in silicon dioxide resistive memory devices. *RSC Adv.* **2015**, *5*, 21215−21236.
(31) Zhou, X.; et al. Study on interface adhesion between phase change material film and SiO2 layer by nanoscratch test. *Jpn. J. Appl. Phys.* **2011**, *50*, 091402.
(32) Thornton, J. a. Influence of substrate temperature and deposition rate on structure of thick sputtered Cu coatings. *J. Vac. Sci. Technol.* **1975**, *12*, 830.
(33) Song, C.; et al. Topological insulator Bi_2Se_3 thin films grown on double-layer graphene by molecular beam epitaxy. *Appl. Phys. Lett.* **2010**, *97*, 143118.
(34) La Torre, A.; Botello-Mendez, A.; Baaziz, W.; Charlier, J.-C.; Banhart, F. Strain-induced metal-semiconductor transition observed in atomic carbon chains. *Nat. Commun.* **2015**, *6*, 6636.
(35) Casari, C. S.; Tommasini, M.; Tykwinski, R. R.; Milani, A. Carbon-atom wires: 1-D systems with tunable properties. *Nanoscale* **2016**, *8*, 4414−4435.

DOI: 10.1021/acs.nanolett.7b00909
Nano Lett. 2017, 17, 3688−3693